Pyrrole as a Probe Molecule for Characterization of Basic Sites in ZSM-5: A Combined FTIR Spectroscopy and Computational Study

Jan Kučera and Petr Nachtigall*

Institute of Organic Chemistry and Biochemistry, Academy of Sciences of the Czech Republic and Center for Complex Molecular Systems and Biomolecules, Flemingovo nám. 2, 166 10 Praha 6, Czech Republic

Josef Kotrla, Gabriela Košová, and Jiří Čejka

J. Heyrovský Institute of Physical Chemistry, Academy of Science of the Czech Republic, Dolejškova 3, 18223 Praha 8, Czech Republic

Received: March 19, 2004; In Final Form: July 30, 2004

The interaction of pyrrole with alkali metal ion exchanged ZSM-5 (Li^+, Na^+, K^+, Rb^+, and Cs^+) was studied by the combination of FTIR spectroscopy and the computational hybrid quantum mechanics/interatomic potential function method describing the role of the aluminum framework content and aluminum distribution, pyrrole coverage, cation size, and cation coordination type. The experimental spectral characteristics were explained using the comparison with the results of computational study. The pyrrole interaction with the metal cation (Lewis acid site) is driven by the pyrrole ring interaction with the metal cation, and it is further stabilized by the formation of a hydrogen bond of the pyrrole NH group with the framework oxygen atom. A large shift of NH vibrations to lower frequencies upon the pyrrole adsorption in M^+/ZSM-5 observed experimentally is almost entirely due to the formation of a hydrogen bond. Two types of the pyrrole NH hydrogen bond were identified: the hydrogen bond to the oxygen atom of the Al−O−Si framework sequence and the hydrogen bond to the oxygen of the Si−O−Si framework sequence. The former type of hydrogen bond shows a larger red shift ($|\Delta\nu| > 150$ cm^{-1}) and corresponds to a broad shoulder in the IR spectra whereas the latter type of hydrogen bond shows a moderate red shift ($80 < |\Delta\nu| < 150$ cm^{-1}) and it corresponds to the band maximum. The shape of the IR spectra depends on the Si/Al ratio, alkali metal ion size, and pyrrole coverage. The combination of experimental and computation approaches brings a new insight into the interaction of pyrrole with alkali metal exchanged ZSM-5 and it provides interpretation of IR spectra at the atomic scale level.

1. Introduction

The alkali metal exchanged zeolites are presently used in separation processes, and their possible use in catalysis of various organic reactions is currently being investigated.[1] Alkali metal exchanged zeolites of different structural types (Y, X, ZSM-5) were tested for their catalytic activity, e.g., in toluene side-chain alkylation with methanol. Solid-state NMR investigation showed that formation of surface bound methoxy groups in Cs−X zeolite plays a crucial role for this alkylation reaction.[2] Using IR spectroscopy Palomares et al. evidenced the key parameters for efficient catalysis of toluene side-chain alkylation in basic zeolites:[3,4] sufficient basic strength to dehydrogenate methanol to formaldehyde, stabilization of sorbed toluene with proper polarization of its methyl group, and balanced sorption stoichiometry of both reactants.

To understand the catalytic activity of alkali metal exchanged zeolites, detailed knowledge about the host−guest complexes between reacting molecules and active sites of zeolite is essential. In the alkali metal exchanged zeolites there are two types of active sites: (i) the alkali metal cations can act as Lewis acid sites and (ii) the zeolite framework oxygen atoms can act as basic sites. The use of a suitable probe molecule represents one of the possibilities for how to characterize the active sites in zeolites and how to obtain more information about the nature of the host−guest interaction. The pyrrole molecule is used for the characterization of alkali metal exchanged zeolites.[5−10] Pyrrole has an amphoteric character, it can interact with both types of active sites: a pyrrole ring interacts with an alkali metal cation and hydrogen of a pyrrole N−H group can form a hydrogen bond (H-bond) with framework oxygen atoms. Both of these effects influence the N−H bond and, therefore, the N−H stretching frequency is changed according to the local environment of the pyrrole adsorption site.[11]

Upon the adsorption in alkali metal exchanged zeolites the pyrrole N−H stretching vibration is shifted to lower frequencies. The pyrrole interaction with aluminum rich zeolites (like Y) was investigated previously.[6,8] IR spectra show a broad peak at 3200−3450 cm^{-1} assigned to the pyrrole N−H stretching vibration. It was shown that the red shift of the N−H vibration depends on the size of the alkali metal and on the Si/Al ratio of the zeolite. It was suggested that the N−H stretching frequency also depends on the local environment of the alkali metal site in zeolite.[6] On the basis of the NMR investigation of zeolite Y, it was concluded that pyrrole preferentially adsorbs on the alkali metal cations located in the SII site in the supercage. The part of the IR spectra corresponding to the N−H stretching vibration was deconvoluted into three peaks corresponding to SII sites

* To whom correspondence should be addressed. E-mail: petr.nachtigall@uochb.cas.cz, phone number: +420 220 410 314.

10.1021/jp048768j CCC: $27.50
Published on Web 09/21/2004

with different numbers of framework aluminum atoms in the six-membered ring. However, no details about the structure of pyrrole−zeolite complex were available. Also, the effect of the pyrrole−pyrrole interaction cannot be ruled out in the case of aluminum-rich zeolites.

To gain a better understanding of the nature of the host−guest interactions, we performed a combined experimental and theoretical investigation of pyrrole interaction with alkali metal ion (Li^+, Na^+, K^+, Rb^+, and Cs^+) exchanged high-silica ZSM-5 zeolite. To maximize the overlap between experimental IR spectroscopy and theoretical computations, the following conditions were maintained: (i) high Si/Al ratio (14 and 33) and (ii) low pyrrole coverage. For such experimental conditions it is assumed that the pyrrole−pyrrole interaction is negligible and single pyrrole molecule can interact with two $M^+/(AlO_4)^-$ sites at most. The interaction of pyrrole with M^+/ZSM-5 was modeled with a combined quantum mechanics/interatomic potential function (QM-pot) method that allows reliable description of pyrrole−zeolite interaction at the density functional theory (DFT) level and that describes the details of the zeolite topology with interatomic potential functions. The following questions were addressed in this combined experimental and theoretical study: (i) what is the nature of the pyrrole/M^+/ZSM-5 interaction, the effect of the cation coordination type, and the effect of the zeolite topology, (ii) how different is the pyrrole interaction with M^+/ZSM-5 in the vicinity of single $M^+/(AlO_4)^-$ unit and in the vicinity of two $M^+/(AlO_4)^-$ units, (iii) what is the effect of the aluminum pair $M^+/(AlO_4)^-\cdots M^+/(AlO_4)^-$ separation on the pyrrole N−H stretching frequency, and (iv) can the information about the aluminum distribution in the zeolite framework be obtained from IR spectra?

Only limited information about the cation positions in the high-silica ZSM-5 is available from the experiment.[12−14] This is partially due to the lack of knowledge on the framework Al distribution. Structure and coordination of alkali metal cations in ZSM-5 was investigated recently by means of the QM-pot method.[14] Only two coordination types of alkali metal cations were found: (i) the sites on top of the six-membered ring on the channel wall (type I sites) and (ii) sites on the channel intersection (type II sites). The relative population of type I and type II sites is determined by the framework Al atom position (unknown from experiments). Nevertheless, for a particular Al position the relative occupation of type I and type II sites depends on the cation size: small Li^+ ion preferably coordinates in type I sites (the strongest Li^+ coordination was found for the six-membered ring with AlO_4 tetrahedron localized in the center of the longer side of the ring) and larger K^+ ion coordinates preferably in type II sites. The Na^+ cations occupy both coordination types.

The interaction of pyrrole with the M^+/X zeolite (aluminum rich system) was investigated using molecular dynamics and Monte Carlo methods followed by Hartree−Fock calculations with cluster models.[8] It was shown that the N−H stretching vibration red shift is caused simultaneously by two types of pyrrole interaction with M^+/zeolite: pyrrole π-system$\cdots M^+$ interaction and formation of the H-bond to zeolite oxygen. A significantly lower N−H stretching frequency (about 130 cm^{-1}) was found for K^+ and Rb^+ ions than for the Na^+ ion.

The interaction of pyrrole with the M^+/high silica zeolite system was recently investigated using cluster models.[11] It was shown that the pyrrole$\cdots M^+$/zeolite complex is dominantly stabilized by the pyrrole π-system interaction with metal cation. The structure of this complex is relatively flexible and it can be further stabilized by the formation of an H-bond between the pyrrole N−H and zeolite framework oxygen atom. It was also shown that the pyrrole π-system$\cdots M^+$ interaction causes only a very small effect on the N−H stretching frequency and this effect almost does not depend on the cation size. The N−H frequency shift is entirely due to the formation of the H-bond. The N−H frequency shift depends on the strength of the H-bond formed which, in turn, depends on the local topology of the zeolite framework (accessibility of the framework oxygen atom). It was concluded that the details of the zeolite framework topology cannot be adequately addressed with cluster models and that more reliable models should be used to describe the interaction of pyrrole with zeolite properly.

2. Methods and Models

2.1. Experimental Section. Two ZSM-5 samples with different Si/Al ratios (14 and 33) were used for the systematic study of the interaction of pyrrole with alkali metal exchanged zeolites. The samples were prepared at the Research Institute for Inorganic Chemistry (Ústí n/L, Czech Republic). The structure of ZSM-5 zeolites was checked by X-ray powder diffraction. No extraframework Al atoms were found in any sample investigated (using FTIR spectroscopy of adsorbed pyridine and ^{27}Al MAS NMR). The zeolite metal forms (Li, Na, K, Rb, Cs) were prepared via repeated ion exchange from the 0.5 M solutions of respective chloride or hydroxide. Ion-exchanged samples were checked by X-ray fluorescence analysis. For Li^+, Na^+, K^+, Rb^+, and Cs^+ ions, ion exchange levels of 100%, 100%, 98%, 96%, and 96%, respectively, were achieved. Pyrrole (Sigma-Aldrich) was distilled under vacuum to obtain a water-free species.

The infrared spectra were recorded on a FTIR Protége 460 Nicolet spectrometer with a resolution of 4 cm^{-1}. The IR spectra (64 scans) were measured in an evacuated apparatus with a MCT/A detector using self-supported wafers of zeolites. Zeolite wafers were prepared under a pressure of 20 kN for several minutes. The sample density varied within 5.8 and 9.4 mg/cm^{-2}. Prior to the experiment, zeolites were activated in situ at 723 K under vacuum for 12 h. All measurements were carried out at room temperature. Before adsorption, pyrrole was degassed by a repeated thawing and freezing method. The experiments were performed as follows: pyrrole was adsorbed at 343 K with a pressure of about 500−550 Pa for 20 min. Desorption was carried out at the same temperature for 30 min. Then the sample was cooled to room temperature and spectra were measured. The second desorption was performed at about 393 K for another 30 min and the spectra were recorded at room temperature. Finally, the IR spectra were recorded at room temperature upon the pyrrole desorption at 443 K.

The amount of adsorbed pyrrole in the individual samples was checked by means of microgravimetric measurements on the CAHN D-101 series balances, following the same condition as in the FTIR experiment.

2.2. Calculations. The system of pyrrole interacting with alkali metal exchanged ZSM-5 (Li^+, Na^+, and K^+ ions) was investigated by the hybrid quantum mechanics/interatomic potential function (IPF) model. This approach combines the ab initio description of part of the system with the interatomic potential function description of the interaction between the remaining atoms (QM-pot model).[15] Within this model the topology of the zeolite framework is fully respected.

In the QM-pot approach the finite inner part describing the site of interest (complex containing pyrrole molecule, alkali metal ions, and sufficiently large surrounding part of ZSM-5 framework) was described at the density functional theory (DFT)

level employing the B3LYP functional[16,17] and a valence triple-ζ-plus-polarization function basis set for O, C, N, Li, Na, and K atoms and with a valence double-ζ-plus-polarization function basis set for Al, Si, and H atoms.[18] The size of the inner part depends on the particular complex structure. To account for all the interactions of the alkali metal cation and pyrrole with the framework, a relatively large inner part was used. Thus, inner parts of sizes from pyrrole/M/$AlSi_6O_{22}H_{16}$ (structure on the intersection, one AlO_4 tetrahedron) to pyrrole/2M/$Al_2Si_9O_{33}H_{22}$ (structure with six-membered ring with part of the intersection edge with two AlO_4 tetrahedra) were used. Oxygen atoms on the edge of the inner part were saturated with the hydrogen atoms (OH termination). The inner part was embedded into the surrounding periodic zeolite framework (outer part). Interactions outside the inner part (outer part) and the cross interactions between the atoms of the inner and outer parts were treated with the core−shell model ion-pair potential with parameters for Si, Al, O, and H atoms taken from ref 19, parameters for Na^+ from ref 20, and parameters for Li^+ and K^+ from ref 14. Intramolecular parameters for the pyrrole molecule were taken from the AMBER package.[21] Parameters from Universal Force Field (UFF) were used for the description of intermolecular interaction of pyrrole molecule with zeolite.[22] It should be noted that the inner part of the QM-Pot model used in this study for the interaction of pyrrole with the surrounding zeolite framework was always sufficiently large to describe this interaction at the B3LYP level and the UFF parameters are used only for the description of the pyrrole interaction with distant atoms of the zeolite framework. Thus, the error due to the use of relatively unreliable UFF parameters is expected to be negligible. The polarizability was taken into account only for O^{2-} anions. Periodic boundary conditions were applied to a unit cell containing 96 T-sites of zeolite framework (95(94) Si atoms, 1(2) Al atom(s)), 192 oxygen atoms, 1(2) atom(s) of the alkali metal, and a single pyrrole molecule). The lattice energy minimization was performed in *P*1 symmetry. No constraints were imposed in the energy minimization.

The interaction energies of pyrrole with the M^+/ZSM-5 system were defined as the energy of reactions:

$$\text{pyrrole} + M^+/\text{ZSM-5} \rightarrow \text{pyrrole}/M^+/\text{ZSM-5}$$

Hence, in addition to the lattice energy minimizations of the pyrrole/M^+/ZSM-5 system the lattice energy minimizations of the M^+/ZSM-5 had to be carried out. At the QM-pot level these geometry optimizations were carried out with the same definition of the inner and outer regions as for the corresponding pyrrole/M^+/ZSM-5 system.

The calculations of N−H stretching frequency shifts were performed at the QM-pot level within the harmonic approximation. It should be noted that the use of harmonic approximation for the description of the hydrogen-bonded system is problematic (for a detailed discussion see section 4).

The calculations were carried out with the QMPOT program,[23] which makes use of the TURBODFT[24] and GULP[25] programs for DFT and shell model potential calculations, respectively. Calculations of vibrational frequencies were made with the GAUSSIAN[26] program suite.

3. Results

3.1. Microgravimetric Measurements. The pyrrole coverage for M^+/ZSM-5 ($M^+ = Li^+$, K^+, and Cs^+) with Si/Al 14 and 33 was investigated by microgravimetry. A pyrrole coverage (θ = pyrrole/M^+) of one molecule on one alkali metal cation was considered as a monolayer (ML). The pyrrole coverages obtained upon the pyrrole desorption at 343 and 443 K are summarized in Table 1.

TABLE 1: Pyrrole Coverage for Li, K, and Cs Exchanged ZSM-5 Samples with Si/Al Ratios 14 and 33 and Temperature of Desorption 343 and 443 K

		θ (pyrrole/M^+)		
T_{des} (K)	Si/Al	Li	K	Cs
343	33	0.6	0.5	0.4
	14	0.6	0.5	0.3
443	33	0.1	<0.1	<0.1
	14	0.2	0.2	0.1

TABLE 2: Pyrrole N−H Stretching Band Maxima for Py/M^+/ZSM-5 (Si/Al = 14, 33) Systems Obtained upon the Pyrrole Desorption at Increasing Temperature of Desorpiton

		ν(N−H) (cm^{-1})				
T_{des} (K)	Si/Al	Li	Na	K	Rb	Cs
343	33	3455	3460	3456	3458	3458
	14	3446	3448	3442	3446	3448
393	33	3446	3452	3454	3456	3456
	14	3446	3448	3442	3444	3448
443	33	3454	3452	3454	3454	3454
	14	3440	3437	3412	3398	3394

It is apparent that the pyrrole coverage did not exceed the monolayer coverage for any sample under the conditions used. Hence, the intermolecular interaction of two or even more pyrrole molecules was not likely to have an effect on the IR spectra. The microgravimetric data obtained for samples upon the desorption at 343 K do not show any dependence of pyrrole coverage on the Si/Al ratio. On the contrary, larger coverage of pyrrole was found for samples with higher Al content after pyrrole desorption at 443 K.

3.2. IR Spectroscopy. The IR spectra of pyrrole adsorbed in the alkali metal exchanged ZSM-5 in the N−H stretching region are shown in Figure 1. The changes in the IR spectra of adsorbed pyrrole were investigated to explain the role of (i) the size of the alkali metal cation, (ii) Si/Al ratio, and (iii) pyrrole coverage (temperature of the pyrrole desorption before IR experiment). A broad band at 3150−3480 cm^{-1} is assigned to the N−H stretching vibration. This vibrations are $|\Delta\nu| = 50-330$ cm^{-1} red-shifted with respect to the gas-phase pyrrole.[8] A band at 3150−3480 cm^{-1} shows a maximum at about 3400−3460 cm^{-1} and a broad shoulder on the lower energy side of the band. With respect to this the band is divided into two parts (Figure 2): area A arround the band maxima (3480−3380 cm^{-1}) and area B covering the band shoulder region (3380−3150 cm^{-1}). The borderline between the two areas is somewhat arbitrary and it will be used only in a qualitative way.

The N−H stretching band maxima for the pyrrole/M^+/ZSM-5 system are summarized in Table 2. The data obtained upon the desorption at 343 and 393 K show only small dependence (about 10 cm^{-1} difference) of the N−H stretching band maximum on the coverage, the cation size and different Si/Al ratio. Similarly, small changes in band maxima were found for Si/Al = 33 and T_{des} = 443 K. Some changes in N−H band maxima were observed only for Si/Al = 14 and desorption temperature 443 K (pyrrole coverage $\theta \leq 0.2$ ML). The increase in the framework Al content was accompanied by the N−H band shift to lower frequencies. This shift increases with the increasing size of the cation (additional N−H shift −14 and −60 cm^{-1} for Li^+ and Cs^+ ions, respectively). The changes in the N−H band maxima obtained for K^+/ZSM-5 systems are also shown in Figure 2.

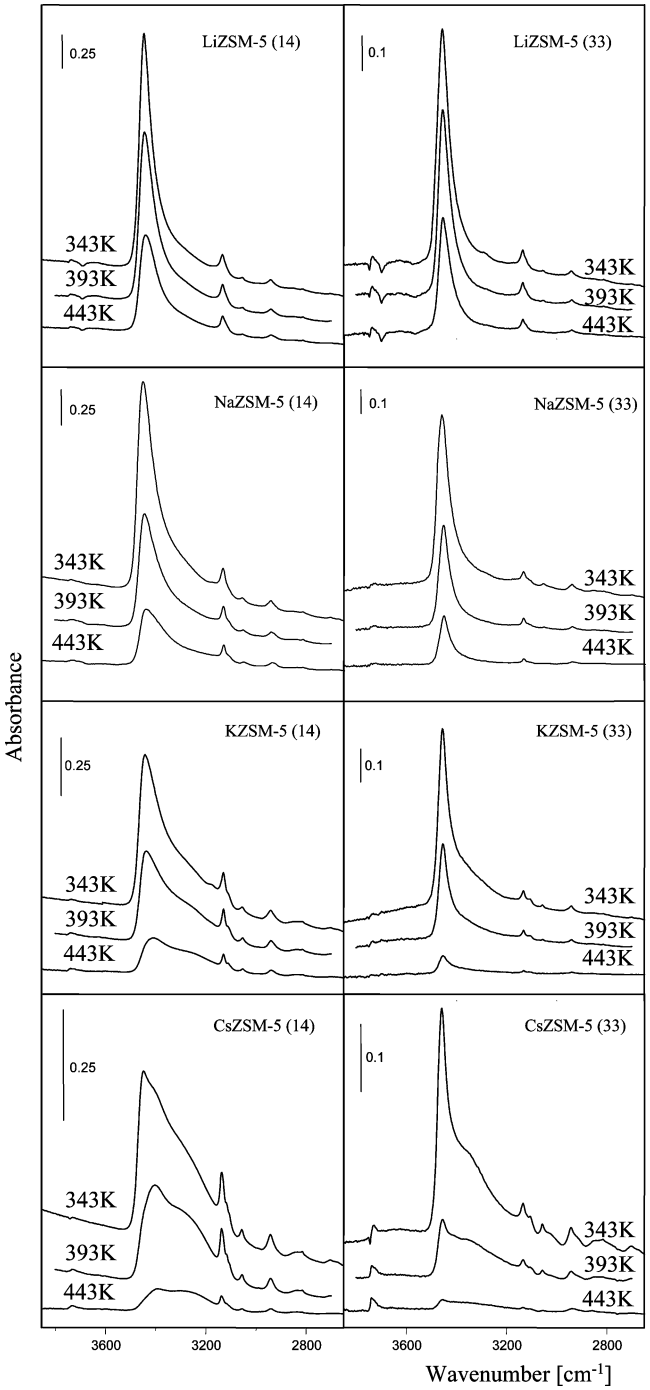

Figure 1. FTIR spectra of pyrrole adsorbed on M^+/ZSM-5 (M^+ = Li^+, Na^+, K^+, and Cs^+) samples with Si/Al ratios 14 and 33. Spectra collected upon the pyrrole desorption at 343, 393, and 443 K.

In contrast to small changes of the positions of N−H maxima a much larger effect on the shape of the spectra due to the variation in the Si/Al ratio, M^+ cation, and pyrrole coverage was observed. It is apparent that the N−H stretching band is nonsymmetrical with a shoulder on the low-energy side of the spectra. The relative population of this shoulder (area B in Figure 2) increases with (i) increasing size of the alkali metal ion, (ii) increasing amount of aluminum in the framework, and (iii) decreasing pyrrole coverage (increasing T_{des}). The effect of the pyrrole coverage and Si/Al ratio on the shape of the IR spectra is also shown in Figure 2 for the K^+/ZSM-5 system. The changes in the shape of the IR band indicate that more than one type of pyrrole adsorption site exists in M^+/ZSM-5. In

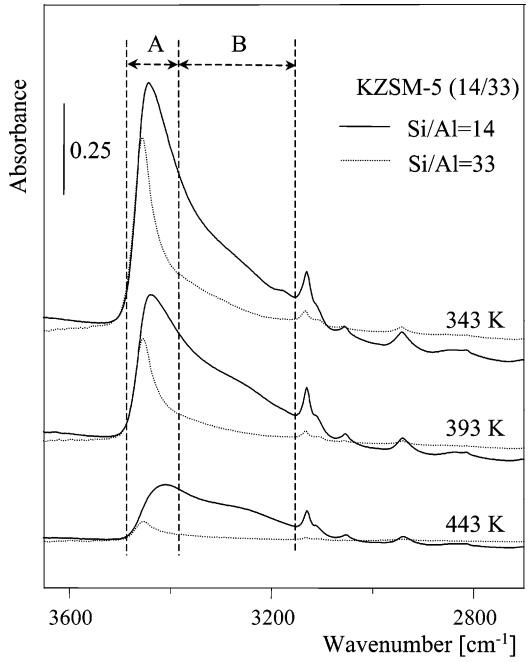

Figure 2. FTIR spectra of pyrrole adsorbed on K^+/ZSM-5 with Si/Al ratios 14 and 33. Spectra collected upon the pyrrole desorption at 343, 393, and 443 K. The N−H stretching band is divided into the band maximum area A and the band shoulder area B.

addition, the changes in the shape of the IR spectra due to the decreasing pyrrole coverage suggest that the adsorption sites with lower frequency are relatively more stable than other pyrrole adsorption sites. Because the shoulder population increases with the increasing content of framework aluminum, it appears that additional $M^+/(AlO_4)^-$ stabilizes the pyrrole adsorption complex.

3.3. Computational Study. Several structures of pyrrole interacting with the M^+/ZSM-5 system were investigated. On the basis of the information of pyrrole interaction with zeolites obtained with the cluster models[8,11] and on the basis of the knowledge of the alkali metal cation sites in ZSM-5,[14] the following pyrrole···M^+/ZSM-5 complexes (Py/M^+/ZSM-5) were studied: (i) Pyrrole interaction with M^+/ZSM-5 in the vicinity of a single $M^+/(AlO_4)^-$ unit. Interaction with an alkali metal cation located on the intersection (type II site) and on top of the six-membered ring (type I site) were considered. The latter case was investigated only for Li^+ and Na^+ cations because the K^+ ion is not expected to occupy this site type.[14] (ii) Pyrrole interaction with M^+/ZSM-5 in the vicinity of two $M^+/(AlO_4)^-$ units located at various positions on the intersection edge.

In all cases, the pyrrole π-system interacts with alkali metal ions and the complex is further stabilized by the H-bond formation between the pyrrole N−H group and the framework oxygen atom. The framework oxygen atoms (considered in this study) with which the pyrrole H-bond can be formed are depicted in Figure 3.

Single $M^+/(AlO_4)^-$ Unit on the Channel Intersection. The pyrrole interaction with a single M^+ cation located on the intersection was considered for two different positions of framework aluminum (T3 and T12 positions; for numbering see ref 27). The pyrrole adsorption energies, the length of H-bond, and the N−H stretching frequency red shifts of adsorbed pyrrole are summarized in Table 3. No structure with H-bond to O_1 or O_2 oxygen atoms was found. To form a stable complex structure, the H-bond must be formed with the framework oxygen atom separated from the AlO_4 tetrahedron by at least two SiO_4

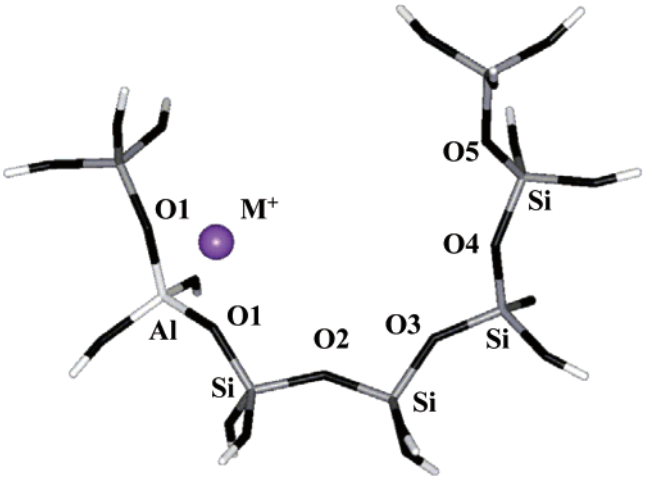

Figure 3. Definition of framework oxygen atom numbering according to the distance from the primary AlO_4 tetrahedron. A part of the ten-membered ring on the channel intersection edge is depicted. The oxygen, silicon, and aluminum are depicted in black, gray, and white, respectively.

TABLE 3: H···O_z H-Bond Lengths,[a] N−H Stretching Frequency Shifts,[c] and Pyrrole Adsorption Energies Calculated for the Pyrrole Interaction in the Vicinity of a Single Framework AlO_4 Tetrahedra (Al at T3 or T12 Positions on the Intersection Edge)

M^+	O_z[a]	H-bond length[b] (Å)	$\lvert\Delta\nu\rvert$[c] (cm^{-1})	E_{ads} (kcal/mol)
		Al in T3 site		
Li^+	O_3	2.04	121	−25.1
	O_4	2.12	87	−25.0
Na^+	O_3	2.05	98	−23.9
	O_4	2.16	66	−23.1
K^+	O_3	2.12	63	−19.9
	O_4	2.44	27	−19.3
		Al in T12 Site		
Li^+	O_3	1.91	177	−26.9
	O_4	1.98	129	−26.6
Na^+	O_3	2.09	89	−22.2
	O_4	2.07	107	−23.8
K^+	O_3	2.07	64	−16.9
	O_4	2.16	57	−17.3

[a] The framework oxygen atom with which the H-bond is formed, AlSiSi−O_3 and AlSiSiSi−O_4 (see Figure 4 for definition). [b] The H-bond length between pyrrole N−H and framework oxygen atom. [c] The N−H stretching red shift with respect to pyrrole gas-phase frequency.

tetrahedra. In the structures considered in this study the pyrrole forms an H-bond with O_3 or O_4 framework oxygen atoms (Figure 3). Complexes with H-bonds to O_3 (Py/M^+/AlSiSi−O_3) and O_4 (Py/M^+/AlSiSiSi−O_4) oxygen atoms (separated by two and three SiO_4 tetrahedra, respectively) are depicted in Figure 4.

The adsorption energy decreases with increasing cation size. The interaction of pyrrole with a single M^+ cation with framework aluminum in T3 position is considered first (upper part of Table 3 and Figure 4). The adsorption energies for both complex structure types (Py/M^+/AlSiSi−O_3 and Py/M^+/AlSiSiSi−O_4) are almost the same for a given cation. However, the H-bond length is larger and the N−H stretching frequency red shift is smaller for complex Py/M^+/AlSiSiSi−O_4 (Figure 4b) than for complex Py/M^+/AlSiSi−O_3 (Figure 4a). The frequency difference between two types of complexes is constant for all alkali metal cations considered (about 32−36 cm^{-1}).

The situation is rather different for framework aluminum in the T12 position. For Li^+ and K^+ ions the larger N−H stretching red shift is found for complex Py/M^+/AlSiSi−O_3 whereas for the Na^+ cation this complex exhibits a smaller red shift. Different frequencies were found for the Py/M^+/ZSM-5 complex when framework aluminum was in the T3 and T12 positions. This difference increases with the decreasing cation size. It is likely that somewhat different N−H stretching frequencies could be found when framework aluminum occupies various positions. The differences in local environment of individual framework positions are responsible for differences in stretching frequencies. The N−H stretching frequencies of pyrrole adsorbed on the Li^+ cation are most affected by the local environment.

Single $M^+/(AlO_4)^-$ Unit on the Six-Membered Ring. Framework aluminum in the T11 position was considered. Only the complex geometries were investigated without performing the frequency calculations. When pyrrole interacts with M^+ on top of the six-membered ring several types of pyrrole···M^+/ZSM-5 complexes can occur: (a) due to the interaction with pyrrole the alkali metal cation is lifted from the ring into the position corresponding to the intersection structure and pyrrole forms an H-bond with the oxygen atom on channel edge (complex A, see Figure 5a); (b) the cation stays coordinated on top of the six-membered ring and pyrrole forms an H-bond with the oxygen atom from the surrounding framework (complex B, see Figure 5b); (c) and the metal cation stays coordinated on top of the six-membered ring and pyrrole forms an H-bond with the oxygen atom of this six-membered ring (complex C). No stable structure of complex C was found. Pyrrole always forms the H-bond to oxygen of the intersection edge (Figure 5). When the Li^+ or Na^+ ion stays coordinated to the six-membered ring (complex B), the M^+···ZSM-5 distance slightly extends (about 0.07 and 0.09 Å for Li^+ and Na^+ ions, respectively) compared to that in the M^+/ZSM-5 system without pyrrole. The pyrrole interaction with M^+/ZSM-5 is weaker for complex B (−17.9 and −21.6 kcal/mol for Li^+ and Na^+, respectively) than for complex A. The difference in adsorption energies on intersection (complex A, Table 3) and on the six-membered ring (complex B) is rather large for Li^+ ion (about 8 kcal/mol). Thus, it is likely that the population of pyrrole in the complex B is significantly lower than for complex A.

Pair of AlO_4 Tetrahedra on the Intersection Edge. Figure 6 depicts the types of the pyrrole···M^+/ZSM-5 complexes in the vicinity of two AlO_4 tetrahedra considered in this study. Both AlO_4 tetrahedra were always situated on the intersection edge. Structures with two AlO_4 tetrahedra separated by 2 and 3 SiO_4 tetrahedra, Al−SiSi−Al (Figure 6a) and Al−SiSiSi−Al (Figure 6b,c), respectively, were investigated. Pyrrole always forms a π-complex with one of the M^+ cations (primary cation charge-compensating a primary AlO_4 tetrahedron) and H-bond to one of the framework oxygen atoms in the vicinity of secondary AlO_4 (charge compensated by the secondary M^+ ion). The pyrrole interaction with the Al−SiSi−Al sequence was studied with primary and secondary AlO_4 tetrahedra in T12 and T2, respectively. The pyrrole interaction with the Al−SiSiSi−Al sequence was studied for primary and secondary AlO_4 tetrahedra in T3 and T2 positions, respectively. A primary cation was always in the intersection site (type II site). Three situations were considered with respect to the position of the secondary cation (see Figure 7): (i) pyrrole forms an H-bond with the framework oxygen (O_b) of the same ring where the secondary M^+ cation is coordinated (M_b^+ secondary ion), (ii) pyrrole forms an H-bond with the framework oxygen (O_b) of a different ring than the secondary M^+ cation is coordinated to (M_n^+ secondary ion), and (iii) the secondary ion interacts with the π-system of pyrrole on the opposite side than primary cation (M_s^+ secondary

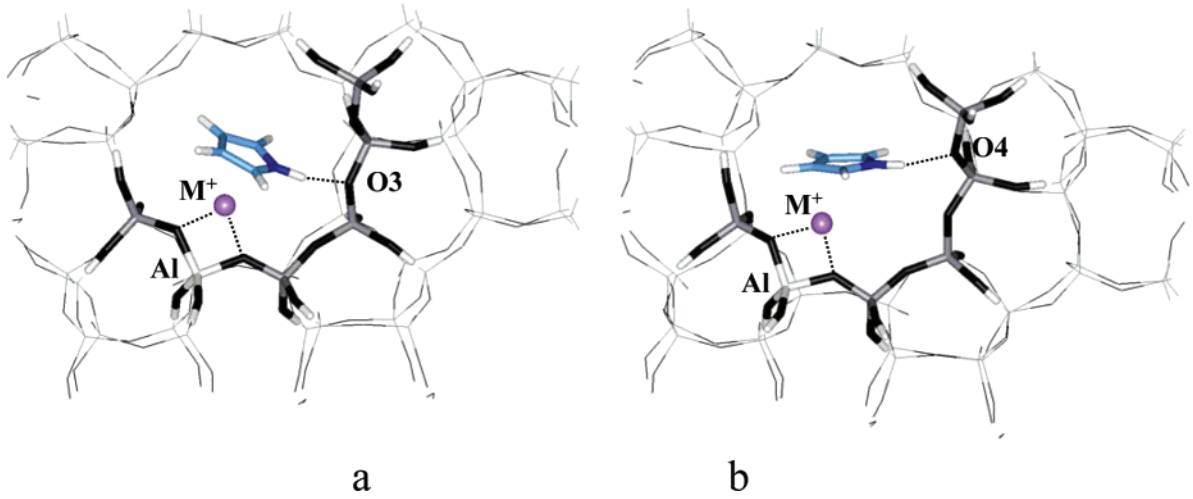

Figure 4. Structure of the pyrrole complex with M^+/ZSM-5 in the vicinity of a single $M^+/(AlO_4)^-$ unit located on the intersection edge: a pyrrole forming an H-bond with the O_3 framework oxygen atom, $Py/M^+/AlSiSi-O_3$ (a); a pyrrole forming an H-bond to the O_4 framework oxygen, $Py/M^+/AlSiSiSi-O_4$ (b).

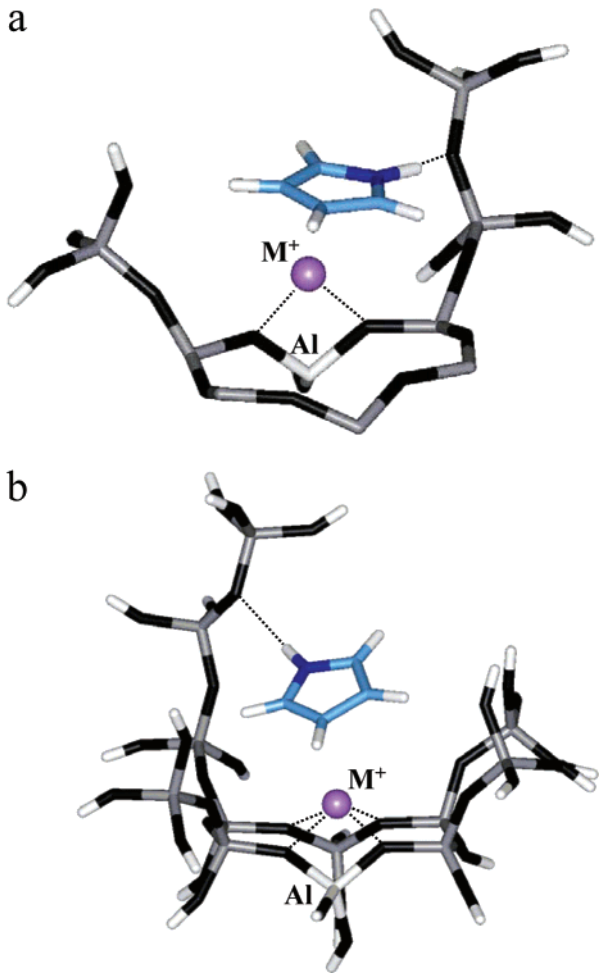

Figure 5. Structure of the pyrrole complex with M^+/ZSM-5 in the vicinity of a single $M^+/(AlO_4)^-$ unit located in the center of a longer side of six-membered ring on the channel wall. A cation is lifted toward the channel intersection upon the pyrrole adsorption, complex A (a), and a cation stays coordinated on top of the six-membered ring upon the pyrrole adsorption, complex B (b).

cation). Calculated pyrrole adsorption energies, the N−H stretching frequency shifts, and the lengths of the pyrrole-framework oxygen H-bonds are summarized in the Table 4.

In the pyrrole complex with the Al−SiSi−Al sequence the H-bond is formed with O_3 framework oxygen atom (Figure 6a).

TABLE 4: H···O_z H-Bond Lengths, N−H Stretching Frequency Shifts, and Pyrrole Adsorption Energies Calculated for the Pyrrole Interaction in the Vicinity of Two AlO_4 Tetrahedra on the Intersection Edge

$Py/2M^+/Al-O(-Si-O)_x$-Al

M^+	complex type[a]	H-bond lengths[b] (Å)	$\|\Delta\nu\|^c$ (cm^{-1})	E_{ads} (kcal/mol)
Li^+	AlSiSiSi−O−Al, M_b^+	1.98	164	−27.1
	AlSiSiSi−O−Al, M_n^+	1.75	396	−29.6
	AlSiSi−O−SiAl[d]	2.02	151	−23.7
	AlSiSi−O−Al, M_b^+	1.88	223	−28.8
	AlSiSi−O−Al, M_n^+	1.60	664	−30.6
Na^+	AlSiSiSi−O−Al, M_b^+	1.91	213	−24.3
	AlSiSiSi−O−Al, M_n^+	1.78	358	−27.4
	AlSiSi−O−SiAl[d]	2.06	130	−24.6
	AlSiSi−O−Al, M_n^+	1.62	591	−25.3
K^+	AlSiSiSi−O−Al, M_b^+	1.86	231	−19.3
	AlSiSiSi−O−Al, M_n^+	1.80	239	−23.3
	AlSiSi−O−SiAl[d]	2.11	93	−21.8
	AlSiSi−O−Al, M_n^+	1.75	321	−17.8

[a] Pairs of framework AlO_4 tetrahedra separated by two and three SiO_4 tetrahedra (AlSiSi−O−Al and AlSiSiSi−O−Al, respectively; see Figure 6 for details). Two types of coordination of the secondary ion, M_b^+ and M_n^+ (see Figure 7 for details), were considered: pyrrole forms an H-bond with the framework oxygen of the same ring where the secondary M^+ cation is coordinated; pyrrole forms an H-bond with the framework oxygen of a different ring than the secondary M^+ cation is coordinated to. [b] The H-bond length between pyrrole N−H and framework oxygen atom. [c] The N−H stretching red shift with respect to pyrrole gas-phase frequency. [d] Pyrrole forms H-bond with framework oxygen of Si−O−Si sequence.

When pyrrole interacts with the Al−SiSiSi−Al sequence the H-bond either to the O_4 framework oxygen (Figure 6c) or to the O_3 framework oxygen (Figure 6b) can be formed. In the former case the H-bond is to the oxygen of the Si−O−Al sequence whereas in the latter case the H-bond is to the oxygen atom of Si−O−Si sequence.

The complex stability, the H-bond length, and thus N−H stretching frequencies, are influenced by several factors. In addition to the factors discussed in the case of the pyrrole complex in the vicinity of a single $M^+/(AlO_4)^-$ unit, the following factors should be considered: (i) type of the framework oxygen atom with which the H-bond is formed (Si−O−Si vs Si−O−Al), (ii) separation of framework Al atoms (Al−SiSi−Al vs Al−SiSiSi−Al), and (iii) coordination type of the secondary ion (M_b^+, M_n^+, or M_s^+).

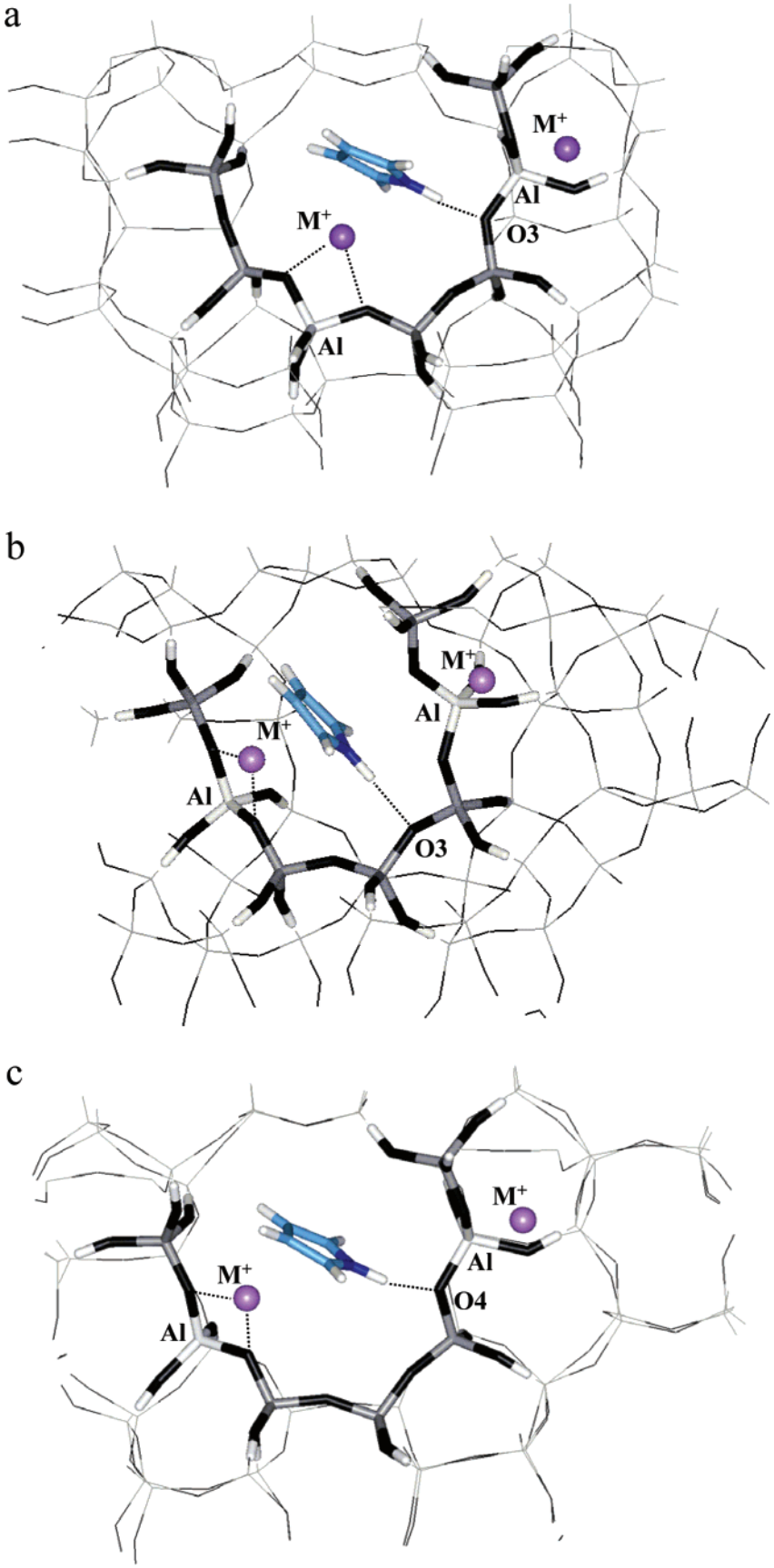

Figure 6. Structure of the pyrrole complex with M^+/ZSM-5 in the vicinity of two $M^+/(AlO_4)^-$ units located on the intersection edge. A pyrrole forms the H-bond to the O_3 framework oxygen atom of the Al−SiSi−Al sequence, Py/M^+/AlSiSi−O_3−Al (a), a pyrrole forms the H-bond to O_3 oxygen atom of Al−SiSiSi−Al sequence, Py/M^+/AlSiSi−O_3−SiAl (b), and a pyrrole forms the H-bond to O_4 oxygen atom of Al−SiSiSi−Al sequence, Py/M^+/AlSiSiSi−O_4−Al (c).

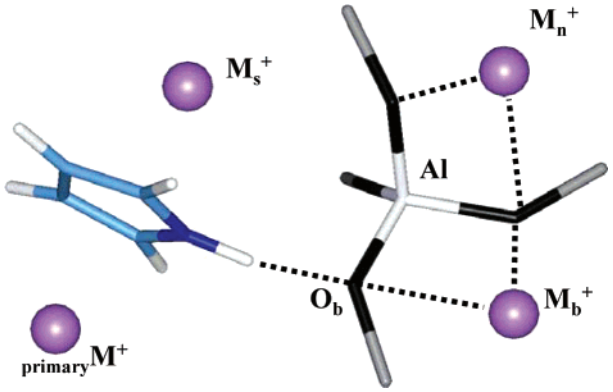

Figure 7. Possible coordinations of the secondary alkali metal cation. The cation compensating the negative charge of the primary AlO_4 tetrahedron is labeled $_{primary}M^+$. The secondary cation coordinated to the π-system of pyrrole on the side of the ring opposite to the primary cation (M_s^+), coordinated to the framework oxygen involved in the H-bond with pyrrole (M_b^+), or coordinated to framework oxygens different from the oxygen forming H-bond (M_n^+).

(i) For a given position of framework Al atoms and for a given type of secondary ion the pyrrole complex with an H-bond to the Si−O−Al framework oxygen is more stable than a complex with an H-bond to the Si−O−Si oxygen atom (by 5.9, 2.8, and 1.5 kcal/mol for Li^+, Na^+, and K^+ ions, respectively). Consequently, the H-bond lengths are shorter and $\Delta\nu$ are more than twice as large for Si−O−Al complexes than for Si−O−Si complexes. The N−H stretching frequencies calculated for the Si−O−Si complex are in the same region as those calculated in the case of a single $M^+/(AlO_4)^-$ unit.

(ii) In the case of the small Li^+ ion the pyrrole complex with the Al−SiSi−Al sequence is more stable than the complex with the Al−SiSiSi−Al sequence (with the difference smaller than 2 kcal/mol). On the contrary, for Na^+ and K^+ ions the complex with the Al−SiSi−Al sequence is less stable than the complex with the Al−SiSiSi−Al sequence (2.1 and 5.5 kcal/mol for Na^+ and K^+ ions, respectively). This is clearly related to the size of the alkali metal cation. For all cations considered, $\Delta\nu$ is considerably larger in the case of the pyrrole complex with the Al−SiSi−Al sequence than the complex with the Al−SiSiSi−Al sequence.

(iii) Surprisingly, a large effect of the coordination of the secondary ion on the N−H stretching frequency was found. The largest N−H stretching red shifts were found for the M_n^+ type of secondary cation. The largest calculated $\Delta\nu$ was found for the M_n^+ secondary ion and the Al−SiSi−Al sequence, −664 and −591 cm^{-1} for Li^+ and Na^+ ions, respectively. This frequency shift appears to be too large comparing to IR data. This situation will be discussed in detail in the next section. In the case of the M_b^+ secondary ion, a significantly smaller $\Delta\nu$ value was found. Smaller $\Delta\nu$ are due to the relative rigidity of the zeolite framework in the vicinity of the secondary ion. The framework oxygen involved in the H-bond (O_b) is less flexible due to the interaction with the secondary M^+ ion. No stable structure with the M_s^+ "stacking" secondary cation was found in this study.

Charge Distribution Analysis. The stability of a particular complex and corresponding N−H stretching frequency shifts can be rationalized in terms of charge distribution analysis for framework oxygen atoms. The charges on the framework oxygen atoms depend on the aluminum atom distribution and on the location of extraframework alkali metal cations. Charges on the framework oxygen atoms are critical for the strength of the pyrrole−zeolite H-bond. A charge distribution on the zeolite oxygen atoms based on the natural bond orbital (NBO)[28] analysis of naked LiZSM-5 cluster is summarized in the Table 5. The NBO charges for a single $M^+/(AlO_4)^-$ unit together with charges for a pair of $M^+/(AlO_4)^-$ units (with M_b^+ and M_n^+ secondary cations) separated by three SiO_4 tetrahedra are presented for framework O_1-O_5 atoms (for notation see Figure 3). In the case of a single $M^+/(AlO_4)^-$ unit the charges on individual oxygen atoms decrease with the increasing distance from the primary Al framework atom. On the basis of the charge distribution analysis, the strongest H-bond could be formed with O_1 or O_2 oxygen atoms. However, formation of such a strong H-bond is accompanied by a large distortion of the M^+/pyrrole complex. Because the interaction between M^+ and the pyrrole π-system is the dominant stabilization interaction, the overall interaction energy between pyrrole and zeolite is smaller when the H-bond to O_1 or O_2 is formed than for complexes with the H-bond to more distant O_3 or O_4 framework oxygen atoms. In fact, a stable structure with the H-bond to O_1 or O_2 oxygen atoms was not found.

TABLE 5: Atomic Charges on the Framework Oxygen Atoms (Natural Bond Orbital Analysis) Calculated for the LiZSM-5 Cluster Model

	O_1	O_2	O_3	O_4	O_5
Al−SiSiSiSi[a]	−1.445	−1.351	−1.311	−1.303	
Al−SiSiSi−Al/M_b^+ [b]	−1.447	−1.299	−1.319	−1.366	−1.369
Al−SiSiSi−Al/M_n^+ [c]	−1.444	−1.312	−1.319	−1.372	−1.443

[a] Isolated framework aluminum atom. [b] Al pair, pyrrole forms H-bond with the framework oxygen of the same ring where the secondary M^+ cation is coordinated. [c] Al pair, pyrrole forms H-bond with framework oxygen of a different ring than the secondary M^+ cation is coordinated to.

The presence of the secondary $M^+/(AlO_4)^-$ units (separated by three SiO_4 tetrahedra from primary AlO_4) leads to a large increase of the negative charge on O_4 and O_5 oxygen atoms. Corresponding to that, stable complexes showing a large N−H vibration shift were found, forming an H-bond to O_4 oxygen atom. The presence of a secondary $M^+/(AlO_4)^-$ unit has only a small effect on the charge on the O_3 oxygen atom. In line with this observation the N−H stretching frequencies are rather similar to the frequencies calculated for a single $M^+/(AlO_4)^-$ unit case.

The position of the secondary M^+ cation has only a small effect on the NBO charges on O_4 oxygen involved in the H-bond. On the contrary, the N−H stretching frequency strongly depends on the position of the secondary ion. It suggests that the differences in N−H stretching frequencies due to the different secondary ion positions are primarily caused by the changes in the flexibility of the framework oxygen involved in H-bond.

4. Discussion

All FTIR spectra in the N−H stretching frequency region (∼3150−3480 cm^{-1}) show a maximum at the high-energy side of the band (∼3400−3460 cm^{-1}). The position of this band is not very sensitive to the cation size, Si/Al ratio, and pyrrole coverage (Figure 1 and Table 2). On the contrary, the shape of this band depends on all these factors. The shape of the spectra will be qualitatively discussed in terms of relative population of band maximum and band shoulder regions (parts A and B in Figure 2, respectively): (i) The band shoulder area relatively increases with increasing temperature of pyrrole desorption. Thus, part B of the spectra is due to the pyrrole adsorption site with higher adsorption energy. (ii) The band shoulder area increases with the increasing content of framework aluminum;

thus, it appears that the pyrrole interaction with more than one $M^+/(AlO_4)^-$ unit increases the adsorption energy. (iii) The intensity of this band shoulder also increases with the increasing cation size. For larger cations the pyrrole interaction with zeolite can be stabilized even with a pair of framework $M^+/(AlO_4)^-$ units at a relatively large distance. At a given thermodynamic condition the overall pyrrole coverage decreases with increasing cation size.

On the basis of the combined QM-pot computational study presented above and on the basis of the previous cluster model study of pyrrole interaction with M^+/ZSM-5,[11] it is apparent that the N−H stretching frequency depends on the formation and the strength of an H-bond between pyrrole and framework oxygen atom. Three different situations may occur: (i) pyrrole forms an H-bond with the oxygen atom adjacent to the secondary framework Al (Al−O−Si oxygen), (ii) pyrrole forms an H-bond with the oxygen atom of the Si−O−Si sequence, and (iii) no hydrogen bond is formed (pyrrole complex stabilized only by interaction of pyrrole ring with cation). The largest N−H stretching frequency red shift ($|\Delta\nu| > 140$ cm^{-1}) was found for pyrrole forming an H-bond with the Al−O−Si oxygen atom. A moderate N−H stretching red shift (57 cm$^{-1} < |\Delta\nu| < 177$ cm^{-1}) was found for pyrrole forming an H-bond with the Si−O−Si oxygen. Only a small red shift ($|\Delta\nu| < 27$ cm^{-1}) was found in the case where no H-bond between pyrrole and the zeolite framework was formed.[11] The complexes without H-bond were found with small cluster models only.[11] When a sufficiently flexible model was used for pyrrole/M^+/ZSM-5 description, the H-bond is always found to stabilize the complex structure. The pyrrole/M^+/ZMS-5 complex with H-bond to this Al−O−Si oxygen atom is 3−5 kcal/mol more stable than the complex with the H-bond to the Si−O−Si oxygen atom. The energy difference slightly decreases with increasing cation size.

Experimental and computational results are in very good qualitative agreement. On the basis of the comparison of these results, the IR spectra can be interpreted at the atomic scale level. Pyrrole adsorbs on the primary alkali metal cation (pyrrole π-orbitals interacts with M^+). This interaction has a dominant stabilization effect,[11] but it has negligible effect on the N−H stretching frequency. In addition to this interaction, pyrrole always forms an H-bond with the framework oxygen atom. The character of the framework oxygen atom forming an H-bond with pyrrole (Si−O−Al or Si−O−Si sequence) has a decisive effect on the strength of the H-bond formed and, thus, on the shift of N−H stretching vibration. The experimental band maximum region ($80 < |\Delta\nu| < 150$ cm^{-1} red-shifted, half-width of this band for Li^+/ZSM-5, Si/Al = 33, and $T_{des} = 343$ K) corresponds to a pyrrole molecule bound at adsorption sites with an H-bond to the Si−O−Si framework oxygen atom. The shoulder of the N−H stretching band ($|\Delta\nu| > 150$ cm^{-1}) corresponds to pyrrole molecules bound at sites with a stronger H-bond to the Al−O−Si framework oxygen atoms.

The predictions drawn on the basis of computational study are in agreement with experimental observations. (i) The region of the band maximum (area A of Figure 2) is dominant in the IR spectra of samples with high Si/Al ratio where the probability of Al pairs in the zeolite framework is small. On the contrary, the shoulder region (area B of Figure 2) dominates the spectra for samples with high framework aluminum content. (ii) At low pyrrole coverage the adsorption sites with the H-bond to the Al−O−Si oxygen (sites with larger adsorption energy) are preferably occupied, corresponding to the IR spectra with a large shoulder. (iii) With increasing ion size, the possibility to form an H-bond with the Al−O−Si oxygen increases. For the small Li^+ cation the structure with the H-bond to the O_3 oxygen is the most stable structure and the relative stability of pyrrole complexes decreases with increasing distance of the framework oxygen involved in this H-bond. For the K^+ ion the complex with the H-bond to the O_4 oxygen is over 5 kcal/mol more stable than the complex with the H-bond to the O_3 oxygen atom. It is likely that for the large Cs^+ cation the complexes with even more distant framework oxygen atoms involved in the H-bond can be stable. Thus, the H-bond with the Al−O−Si oxygen for distant secondary AlO_4 is possible for large cations but it is not likely for small cations. As a result, the shoulder intensity in the IR spectra increases with the increasing ion size. (iv) The experimental N−H stretching band is very broad due to the large complexity of the M^+/ZSM-5 system (different local topology for particular framework aluminum position and a broad distribution of framework aluminum pairs). The broadness of the band maximum area is related to differences between structures with the H-bond to the Si−O−Si framework oxygen atom. In the case of a single $M^+/(AlO_4)^-$ unit, it was shown that the N−H stretching frequencies differ appreciably when the Al atom is at different framework positions. The difference reflecting the effect of the local topology is largest for small Li^+ ion (50 cm^{-1}) and it decreases with the increasing ion size. The N−H stretching frequency corresponding to the H-bond with the Si−O−Si oxygen can be further modified (by about 20 cm^{-1}) due to changes of the framework oxygen charges caused by the presence of distant secondary framework aluminum. A large broadness of band shoulder is related to differences among the complex structures with the H-bond to Al−O−Si. Rather different N−H stretching frequencies were found for Al pairs separated by two and three SiO_4 tetrahedra. In addition, the type of secondary cation coordination has a large effect on the N−H frequencies. It is assumed that the local topology of particular framework aluminum positions has a similar effect as in the case of a single $M^+/(AlO_4)^-$ unit.

One of the goals of this study was to find whether the pyrrole probe molecule can bring some information about the framework aluminum pair distribution. As discussed above, there is a large variety of possible pyrrole···M^+/ZSM-5 complex types. Pyrrole adsorption energies in many sites are rather similar (only few kcal/mol difference); thus, the population of these sites should also be considered. From the relative population of band maxima and band shoulder, qualitative information about the existence of the framework aluminum pairs can be obtained. However, Al pairs separated by two, three, or even four SiO_4 tetrahedra cannot be distinguished from the IR spectra. We conclude that meaningful information about Al pairs can be obtained only for the smallest cation (Li^+) and zeolites with very high Si/Al ratios.

For some structures a very large N−H stretching frequency shift (~600 cm^{-1}) was found. These are larger than observed experimentally. However, the pyrrole···M^+/ZSM-5 complex with such a large shift was found only for a particular position of two framework aluminum atoms. It is likely that the population of these structures is very low and cannot be detected experimentally.

All the calculations of N−H stretching frequencies performed in this study were done within the harmonic approximation. We are aware that this approximation is rather crude for the description of vibrational dynamics of H-bonded systems. However, we believe that for a qualitative description of the IR spectra of pyrrole adsorbed in M^+/ZSM-5 system the harmonic approximation is acceptable. For calculations of frequency shifts the anharmonic correction partially cancels out.

It is expected that the effect of anharmonicity is larger for H-bonded complex; thus, $\Delta\nu$ computed within the harmonic approximation should be underestimated.

Interaction of pyrrole with alkali metal exchanged zeolite Y was thoroughly investigated by Sanchez-Sanchez and Blasco using the combination of NMR and IR techniques.[6] They observed the changes in the alkali metal coordination upon the adsorption of pyrrole. The IR spectra in the N−H stretching region were interpreted as the superposition of several bands. Individual bands were assigned to adsorption sites with different basicities, suggesting that the six-membered ring with one, two, and three Al atoms can be distinguished from the IR spectra.

Interaction of pyrrole with alkali metal exchanged zeolite X was recently investigated computationally by means of DFT and the small cluster model.[29] The SIII site was modeled with the $M^+/AlSi_5O_7H_{10}$ cluster model (two adjacent four-membered rings). It was found that pyrrole preferably binds only to M^+ (π-interaction) without the pyrrole···framework hydrogen bond. This result appears to be in contradiction with the result of the computational study presented above. In fact, it is only a seeming contradiction: we were not able to find an H-bond stabilized structure of complex C (pyrrole adsorbed on the M^+ site on the six-membered ring with an H-bond to the oxygen atom of this six-membered ring, see section 3.3). This is a rather similar situation, as studied in the work of Correa where only oxygen atoms in the model are in the ring.[29] However, we were able to find complexes A and B stabilized by the H-bond formation (see section 3.3 and Figure 5) where the H-bond is formed with the framework oxygen atom from outside the six-membered ring occupied by the M^+ ion. Thus, we believe that the conclusion drawn by Correa is not correct and it only results from the use of insufficient cluster model. All the conclusions drawn in ref 29 are then questionable. Förster et al. used the Hartree−Fock method and four-membered ring cluster model to describe the pyrrole interaction with M^+ in SII site in faujasite. In agreement with our result they found that the N−H stretching frequency shift is due to the H-bond formation between pyrrole N−H and framework oxygen atom. In their model the four-membered ring represents the part of the zeolite framework interacting with the pyrrole N−H group whereas the alkali metal cation is not properly coordinated to the framework.

5. Conclusion

The pyrrole interaction with alkali metal exchanged high-silica ZSM-5 was investigated by a combination of experimental IR and computation QM-pot investigation. IR spectra of pyrrole absorbed on M^+/ZSM-5 ($M^+ = Li^+$, Na^+, K^+, Rb^+, and Cs^+) for samples with Si/Al ratio 33 and 14 were measured for various pyrrole coverages (T_{des} = 343, 393, and 443 K). The red shift of the pyrrole N−H stretching vibration is interpreted on the basis of the computation of pyrrole complexes with M^+/ZSM-5 at QM-pot level. Pyrrole complexes in the vicinity of a single AlO_4 and in the vicinity of two AlO_4 tetrahedra at increasing distance were investigated in the computational part.

Two effects participate in the pyrrole···M+/ZSM-5 interaction. A dominant stabilization comes from the pyrrole ring π-system interaction with the cation and the complex is farther stabilized by the formation of an H-bond between the hydrogen of the N−H group and a framework oxygen. The strength of this H-bond has a major effect on the NH stretching red shift. A broad N−H stretching band observed in the IR spectra in the 3150−3480 cm^{-1} region shows a maxima at about 3400−3460 cm^{-1} and a broad shoulder on the lower energy side of the band. The band maximum ($80 > |\Delta\nu| > 150$ cm^{-1} red-shifted) corresponds to the complexes in which pyrrole forms the H-bond with the Si−O−Si framework oxygen atoms. The band shoulder ($|\Delta\nu| > 150$ cm^{-1}) corresponds to the complex in which the pyrrole molecule forms a stronger H-bond to the more basic framework oxygen of the Al−O−Si sequence. The band maximum (~3455 cm^{-1}) does not depend on the cation size, Si/Al ratio, and pyrrole coverage. On the contrary, the shape of the spectra depends on these effects. The population of band shoulder depends on the probability of the formation of a pyrrole H-bond with the framework oxygen atom of the Si−O−Al sequence. The population of the band shoulder increases (i) with the increasing cation size (the possibility to form an H-bond with a framework oxygen further from the primary framework Al increases), (ii) with the decreasing Si/Al ratio, and (iii) with the decreasing pyrrole coverage (complexes with an H-bond to the oxygen of the Si−O−Al sequence are more stable than complexes with an H-bond to the oxygen of the Si−O−Si sequence).

Acknowledgment. We thank the Czech Ministry of Education for support for the Center for Complex Molecular Systems and Biomolecules, Grant No. LN00A032 (J.K., P.N.), the Grant Agency of the Academy of Sciences of the Czech Republic, A4040001 (J.C., J.K., and G.K.), and the Volkswagen-Stiftung, I/75 886 (J.C.). Also we thank Julian Gale for the GULP code, and Marek Sierka and Joachim Sauer for providing the QM-pot code.

References and Notes

(1) Barthomeuf, D. *Catal. Rev.-Sci. Eng.* **1996**, *38*, 521.
(2) Philippou, A.; Anderson, M. W. *J. Am. Chem. Soc.* **1994**, *116*, 5774.
(3) Palomares, A. E.; Eder-Mirth, G.; Lercher, J. A. *J. Catal.* **1997**, *168*, 442.
(4) Palomares, A. E.; Eder-Mirth, G.; Rep, M.; Lercher, J. A. *J. Catal.* **1998**, *180*, 56.
(5) Sanchez-Sanchez, M.; Blasco, T. *Chem. Commun.* **2000**, 491.
(6) Sanchez-Sanchez, M.; Blasco, T. *J. Am. Chem. Soc.* **2002**, *124*, 3443.
(7) Murphy, D.; Massiani, P.; Franck, R.; Barthomeuf, D. *J. Phys. Chem.* **1996**, *100*, 6731.
(8) Forster, H.; Fuess, H.; Geidel, E.; Hunger, B.; Jobic, H.; Kirschhock, C.; Klepel, O.; Krause, K. *Phys. Chem. Chem. Phys.* **1999**, *1*, 593.
(9) Huang, M.; Adnot, A.; Kaliaguine, S. *J. Catal.* **1992**, *137*, 322.
(10) Barthomeuf, D. *Microporous Mesoporous Mater.* **2003**, *66*, 1.
(11) Kucera, J.; Nachtigall, P. *Collect. Czech. Chem. Commun.* **2003**, *68*, 1848.
(12) Olson, D. H.; Khosrovani, N.; Peters, A. W.; Toby, B. H. *J. Phys. Chem. B* **2000**, *104*, 4844.
(13) Accardi, R. J.; Lobo, R. F. *Microporous Mesoporous Mater.* **2000**, *40*, 25.
(14) Kucera, J.; Nachtigall, P. *Phys. Chem. Chem. Phys.* **2003**, *5*, 3311.
(15) Eichler, U.; Kolmel, C. M.; Sauer, J. *J. Comput. Chem.* **1997**, *18*, 463.
(16) Becke, A. D. *J. Chem. Phys.* **1993**, *98*, 5648.
(17) Lee, C. T.; Yang, W. T.; Parr, R. G. *Phys. Rev. B—Condens. Matter* **1988**, *37*, 785.
(18) Schafer, A.; Horn, H.; Ahlrichs, R. *J. Chem. Phys.* **1992**, *97*, 2571.
(19) Sierka, M.; Sauer, J. *Faraday Discuss.* **1997**, 41.
(20) Jackson, R. A.; Catlow, C. R. A. *Mol. Simul.* **1988**, *1*, 207.
(21) Pearlman, D. A.; C. D. A.; Caldwell, J. W.; Ross, W. S.; Cheatham, T. E., III; Ferguson, D. M.; Seibel, G. L.; Singh, U. C.; Weiner, P. K.; Kollman, P. A. Amber 4.1., University of California, San Francisco, CA, 1995.
(22) Rappe, A. K.; Casewit, C. J.; Colwell, K. S.; Goddard, I. W. A.; Skiff, W. M. *J. Am. Chem. Soc.* **1992**, *114*, 10024.
(23) Sierka, M.; Sauer, J. *J. Chem. Phys.* **2000**, *112*, 6983.
(24) Treutler, O.; Ahlrichs, R. *J. Chem. Phys.* **1995**, *102*, 346.
(25) Gale, J. D. *J. Chem. Soc.-Faraday Trans.* **1997**, *93*, 629.
(26) Frisch, M. J.; Trucks, G. W.; Schlegel, H. B.; Scuseria, G. E.; Robb, M. A.; Cheeseman, J. R.; Montgomery, J. A., Jr.; Vreven, T.; Kudin, K. N.; Burant, J. C.; Millam, J. M.; Iyengar, S. S.; Tomasi, J.; Barone, V.; Mennucci, B.; Cossi, M.; Scalmani, G.; Rega, N.; Petersson, G. A.;

Nakatsuji, H.; Hada, M.; Ehara, M.; Toyota, K.; Fukuda, R.; Hasegawa, J.; Ishida, M.; Nakajima, T.; Honda, Y.; Kitao, O.; Nakai, H.; Klene, M.; Li, X.; Knox, J. E.; Hratchian, H. P.; Cross, J. B.; Adamo, C.; Jaramillo, J.; Gomperts, R.; Stratmann, R. E.; Yazyev, O.; Austin, A. J.; Cammi, R.; Pomelli, C.; Ochterski, J. W.; Ayala, P. Y.; Morokuma, K.; Voth, G. A.; Salvador, P.; Dannenberg, J. J.; Zakrzewski, V. G.; Dapprich, S.; Daniels, A. D.; Strain, M. C.; Farkas, O.; Malick, D. K.; Rabuck, A. D.; Raghavachari, K.; Foresman, J. B.; Ortiz, J. V.; Cui, Q.; Baboul, A. G.; Clifford, S.; Cioslowski, J.; Stefanov, B. B.; Liu, G.; Liashenko, A.; Piskorz, P.; Komaromi, I.; Martin, R. L.; Fox, D. J.; Keith, T.; Al-Laham, M. A.; Peng, C. Y.; Nanayakkara, A.; Challacombe, M.; Gill, P. M. W.; Johnson, B.; Chen, W.; Wong, M. W.; Gonzalez, C.; Pople, J. A. *Gaussian 03*, revision B.01; Gaussian, Inc.: Pittsburgh, PA, 2003.

(27) van Koningsveld, H.; Jansen, J. C.; van Bekkum, H. *Zeolites* **1990**, *10*, 235.

(28) Reed, A. E.; Weinhold, F.; Curtiss, L. A.; Pochatko, D. J. *J. Chem. Phys.* **1986**, *84*, 5687.

(29) Correa, R. J. *Tetrahedron Lett.* **2003**, *44*, 7299.